Current-Induced Torques Due to Compensated Antiferromagnets

Paul M. Haney and A. H. MacDonald
Department of Physics, The University of Texas at Austin, Austin, Texas, 78712-0264, USA
(Received 23 August 2007; published 12 May 2008)

We analyze the influence of current-induced torques on the magnetization configuration of a ferromagnet in a circuit containing a compensated antiferromagnet. We argue that these torques are generically nonzero and determine their form by considering spin-dependent scattering at a compensated antiferromagnetic interface. Because of symmetry dictated differences in the form of the current-induced torque, the phase diagram which expresses the dependence of the ferromagnetic configuration on the current and external magnetic field differs qualitatively from its ferromagnet-only counterpart.

DOI: 10.1103/PhysRevLett.100.196801 PACS numbers: 85.35.−p, 72.25.−b

Introduction.—Current-induced torques in noncollinear ferromagnetic metal circuits were predicted over 10 years ago [1,2], and have since been the subject of an extensive and quite successful body of experimental and theoretical research [3]. Almost all studies of current-induced torques consider either their role in ferromagnetic (F) spin-valve circuits [4–8] or their influence on magnetic domain wall motion [9–13]. In both cases, the current-induced torques can be understood as following from the transfer of conserved spin angular momentum from current-carrying quasiparticles to the magnetic condensate. The total current-induced torque acting on a F nanoparticle can be expressed in terms of the difference between incoming and outgoing spin currents [1]. The spin current in a F layer becomes aligned with the magnetization within a few lattice constants of the interface [14], so that the net spin-current flux and ensuing current-induced torque can be found by computing spin currents at the interface alone.

It has recently been predicted that current-induced torques are generically present whenever nonequilibrium quasiparticles interact with noncollinear magnetic order parameters, even [15,16] in circuits containing only antiferromagnetic (AF) elements. Experiments [17] have established a dependence of unidirectional exchange bias fields on current, providing indirect evidence that current-induced torques are present in AFs, but the absence of a simple conservation law constraint makes quantitative comparisons between theory and experiment much more challenging than in the ferromagnetic case. Achieving quantitative control and understanding of the interrelated current-induced torques which act on the moments of both ferromagnetic and antiferromagnetic circuit elements would enrich the palette of spintronics, potentially offering advantages for applications [18].

In this Letter we analyze the influence of the current-induced torques acting on a F thin film in a circuit containing a compensated AF. Because of a key difference in symmetry compared to purely F spin-valve circuits, we find that the phase diagram which expresses the dependence of the magnetic configuration of the F on current and external magnetic field differs qualitatively from the familiar F-only spin-valve phase diagram [19]. In particular, we find that transport currents can drive the F to a stable steady state with magnetization perpendicular to the AF layer moments. The proposal here offers unique qualitative predictions of current-induced torques arising from AF which should be robust to system imperfections, such as multidomain AF structure.

Symmetry considerations.—For this simplified analysis, we treat F simply as a source of current polarized along $\hat{n}_F$, and consider scattering at the interface with a compensated AF with moment orientation $\hat{n}_{\rm AF}$ (see Fig. 1). Because the effective magnetic field in the quasiparticle Hamiltonian of the AF will in general have components perpendicular to $\hat{n}_{\rm F}$, scattering off the AF can flip spins, leading to spin currents transverse to $\hat{n}_{\rm F}$ and hence to a current-induced torque acting on the F. Invariance under global spin rotations when spin-orbit interactions are negligible places powerful restrictions on the form of the torque. Global rotations by 180 degrees about an axis in the plane of $\hat{n}_{\rm F}$ and $\hat{n}_{\rm AF}$ invert the angle θ between the two directions. It follows that the torque on the ferromagnet must be an odd function of θ and therefore expandable in terms of a sine-only Fourier series, vanishing for parallel and antiparallel orientations. In a compensated AF, reversal of the AF moment direction is equivalent to a lateral translation which cannot influence the current-induced torque. It fol-

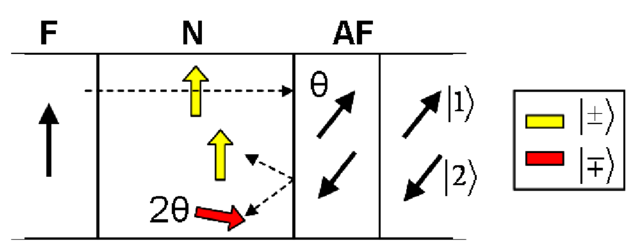

FIG. 1 (color online). Spin-dependent reflection of an incident electron with sublattice state $\gamma = |\pm\rangle$ and spin $|\uparrow\rangle$ at a compensated AF interface with moment orientation θ. Scattering which preserves the sublattice state (light arrow) also preserves spin, while scattering between γ channels (dark arrow) results in spin-rotation by 2θ.

lows that in the compensated AF case the torque is also invariant under $\theta \to \theta + \pi$, restricting its Fourier expansion to terms proportional to $\sin(2n\theta)$. The torque therefore also vanishes when $\hat{n}_{\rm F}$ is perpendicular to $\hat{n}_{\rm AF}$, and undergoes a sign change for $\theta \to \pi - \theta$. The property that the current-induced torque acting on a F due to a compensated AF vanishes not only for collinear but also for perpendicular orientations is primarily responsible for the novel current-induced torque phase diagram that we discuss later.

Spin-dependent scattering from a compensated AF.—We now present a more microscopic, but still qualitative, discussion of current-induced torques due to scattering from a compensated AF. For definiteness we consider electron flow from F to AF through a normal (N) metal spacer and focus on the reflection of spin-polarized flux from a compensated AF interface. The reflected spin-current flux determines the torque on F (see Fig. 1).

A simple compensated AF has a bipartite lattice with two sublattice sites (labeled $|1\rangle$ and $|2\rangle$ in Fig. 1). The local quasiparticle Hamiltonian on these sites differs only in the sign of the effective magnetic field. It is instructive to expand wave functions for both F and AF in the basis $|\pm\rangle = (|1\rangle \pm |2\rangle)/\sqrt{2}$. Scattering at a N/AF interface then has four channels: (γ, σ) where $\gamma = (+, -)$, $\sigma = (\uparrow, \downarrow)$, and reflection and transmission are described by 4×4 matrices. The crucial point is that spin-flip scattering occurs *if and only if* the sublattice state is also flipped between $|+\rangle$ and $|-\rangle$ states. This property follows from the invariance of the AF Hamiltonian under the combined operations of sublattice interchange ($|1\rangle \leftrightarrow |2\rangle$) and time reversal [20]. This observation can be motivated by noting that *only* the spin-dependent effective magnetic field term mixes $|+\rangle$ and $|-\rangle$.

Let $r^{\gamma\gamma'}_{\sigma\sigma'}$ denote the amplitude for an incident state $|\gamma, \sigma\rangle$ to be reflected into state $|\gamma', \sigma'\rangle$. From the above analysis, the spin dependence of the reflection coefficients can be expressed explicitly: $r^{\pm,\pm}_{\sigma,\sigma'} = r^{\pm,\pm}\delta_{\sigma,\sigma'}$ and $r^{\pm,\mp}_{\sigma,\sigma'} = r^{\pm,\mp}(\hat{n}_{\rm AF} \cdot \tau_{\sigma,\sigma'})$, where τ is a vector of Pauli spin matrices. Scattering that preserves γ is spin independent, while scattering from one γ channel to another is due entirely to an effective magnetic field along $\hat{n}_{\rm AF}$. We take $\hat{n}_F = \hat{z}$, $\hat{n}_{\rm AF} = \sin(\theta)\hat{x} + \cos(\theta)\hat{z}$, and consider incoming spin-polarized eigenstates of N with momentum $k_\parallel$ transverse to the direction of current flow. For $k_\parallel = 0$, the incoming state is $|+, \uparrow\rangle$, and the reflected state is $\psi_r = r^{++}|+, \uparrow\rangle + r^{+-}[\cos(\theta)|-, \uparrow\rangle + \sin(\theta)|-, \downarrow\rangle]$. Since $\langle +|v|-\rangle = 0$ where v is the current-direction velocity operator, it follows that the reflected spin-current is proportional to

$$\mathbf{Q} = R^{++}\mathbf{z} + R^{+-}[\cos(2\theta)\mathbf{z} + \sin(2\theta)\mathbf{x}], \qquad (1)$$

where $R^{\gamma\gamma'} = |r^{\gamma\gamma'}|^2$. Figure 1 illustrates the separate spin dependence of the two γ scattering channels. For $k_\parallel \neq 0$, the incident state is a linear combination of $|+\rangle$ and $|-\rangle$, and the reflected spin current contains terms proportional to $\sin(2\theta)$ and $\sin(\theta)$; however, the $\sin(\theta)$ term is canceled exactly by the state with wave vector $-k_\parallel$ [21]. The spin currents and ensuing torques satisfy the symmetry requirements discussed in the previous section. The presence of the F layer in the circuit will induce a spin-polarized current, and the component of the spin current noncollinear with the AF director will be deflected as described above. Since the current-induced torque is proportional to the component of spin current transverse to the F (in this case the $\mathbf{x}$ direction), the angular dependence of the current-induced torque is of $\sin(2\theta)$ form, in contrast to the conventional $\sin(\theta)$ form. A similar analysis holds for electron flow from AF to F.

We have performed detailed *ab initio* transport calculations for an AF-F interface between antiferromagnetic NiMn and ferromagnetic Co, using the geometry described in Ref. [22], calculating the current-induced torque using the methods of Ref. [23]. These calculations, which will be detailed in a subsequent paper, produce a current-induced torque with the $\sin(2\theta)$ angle dependence predicted here on the basis of general arguments. To determine the current-induced torque present on the AF layer, calculating incoming spin currents is no longer sufficient [15], so that the previous analysis does not apply. We find nevertheless that the angular dependence is again of the $\sin(2\theta)$ form by adding the torques on individual atoms in the AF lattice. The same qualitative results are found for mean-field calculations on toy model lattice systems with on-site electron-electron interactions.

The current-induced torque tends to drive the orientation of downstream material (AF or F) parallel to that of the upstream, and to drive the upstream material orientation perpendicular to the downstream (so that for electron flow from AF to F, the F tends to align to AF, and the AF tends to become perpendicular to F, within their common plane).

Phase diagram for a pinned antiferromagnet.—We now consider the implications of this new form of current-induced torque for systems with the usual thin film geometry, assuming for the sake of definiteness that the AF moment director $\hat{n}_{\rm AF} = \pm\hat{z}$ is pinned and lies in the plane, and that the external magnetic field H is applied along the same axis. We use a spherical coordinate system for the F moment direction, taking $\hat{n}_{\rm AF}$ as the polar direction and the $\hat{x}$ direction as the film normal. We assume that a nonmagnetic spacer layer is placed between the F and AF layers which is sufficiently wide to make exchange interactions negligible. We also omit easy-axis anisotropy; its inclusion would not substantially change the picture described below. With these ingredients the polar and azimuthal torques acting on the ferromagnet are

$$\Gamma_\theta = -\frac{1}{2}\sin(\theta)\sin(2\phi)H_d + \sin(2\theta)H_{CI},$$
$$\Gamma_\phi = \sin(\theta)H + \frac{1}{2}\sin(2\theta)\cos^2(\phi)H_d. \qquad (2)$$

Here we have parametrized the current-induced torque by H_{CI} and chosen a sign convention in which $H_{CI} < 0$ when it favors perpendicular alignment. H_d denotes the demagnetizing field. Steady-state solutions satisfy $\Gamma_\phi = \Gamma_\theta = 0$

and are stable for small deviations when Gilbert damping is included. We have determined the stability regions of the steady-state solutions discussed below by following the procedure described in Ref. [24]. We present all of our results in terms of the dimensionless fields $h = H/H_d$ and $h_{CI} = H_{CI}/H_d$.

For the geometry we consider, the behavior of F is very simple in the absence of the current-induced torques: the magnetization simply lines up with the magnetic field applied in the easy plane. The influence of the current-induced torque on F is particularly dramatic for $H_{CI} < 0$. Because the torques then tend to push the magnetization perpendicular to $\hat{n}_{\mathrm{AF}}$, the field-aligned solution loses stability for

$$|h_{CI}| \geq \frac{\alpha}{2}\left(|h| + \frac{1}{2}\right), \tag{3}$$

where α is the Gilbert damping parameter. For sufficiently strong currents and external fields that are not too strong, a perpendicular-to-plane steady state becomes stable:

$$\theta = \frac{\pi}{2} + h, \qquad \phi = -2h_{CI}h + n\pi. \tag{4}$$

These equations have been derived assuming that h and h_{CI} are small. In the above n is an even integer for solutions which point approximately in the $+\hat{x}$ direction, and an odd integer for the $-\hat{x}$ direction. The region of stability for this solution is

$$|h_{CI}| \geq \frac{\alpha}{2}\left(\frac{h\sin h - 2\cos^2 h}{h\sin h - \cos 2h}\right), \tag{5}$$

where the denominator on the right-hand side of the above inequality must be less than 0, implying that $|h| < 0.608$, or equivalently $|H| < \mu_0 M_s(0.608)$. Again, Eqs. (3) and (5) are for $h_{CI} < 0$.

The stability of the counter-intuitive stable steady state given by Eq. (4) is explained in Fig. 2. This figure illustrates the situation when the excursions from the easy plane are small. For simplicity we first consider no external field. In the absence of the current-induced torque a small fluctuation out of the easy plane would initiate precession about the hard axis which damps back into the easy plane. The presence of the $\sin 2\theta$ torque, however, drives the magnetization perpendicular to $\hat{n}_{\mathrm{AF}}$ within their common plane. As the magnetization orientation $\hat{m}$ precesses around the hard axis, this torque vector has a component

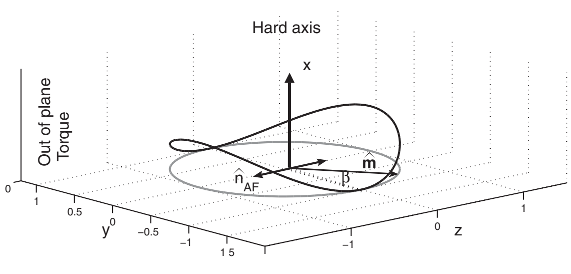

FIG. 2. Saddle shape illustrates the out-of-plane torque vs β for small excursions of the magnetization orientation $\hat{m}$ from the easy plane. The out-of-plane torque is always positive.

which points out of the easy plane. If the angle between $\hat{n}_{\mathrm{AF}}$ and the in-plane component of $\hat{m}$ is β, the magnitude varies as $\Gamma_x = 2H_{CI}m_x\sin^2\beta$, as shown in the figure. The crucial point is that this torque is always positive throughout the precession. When this torque exceeds the damping, the out-of-plane configuration is stabilized. The eventual out-of-plane orientation can be $+\hat{x}$ or $-\hat{x}$ depending on the direction of the initial fluctuation out-of-plane. The presence of an applied field changes the trajectory of the magnetization upon excursions from the easy plane. For a sufficiently large applied field, the torque is unable to stabilize the out-of-plane configuration, and no steady state is reached.

Interesting new steady states can in principle also be induced by the current-induced torque for $H_{CI} > 0$. For $|H| \leq H_d$, the steady-state stability analysis identified configurations in which the magnetization is approximately antialigned with the applied field:

$$\theta = \cos^{-1}(-h), \qquad \phi = -2h_{CI}h, \tag{6}$$

which is stable for the range of applied fields and currents

$$h_{CI} \geq \frac{\alpha}{2}\left(\frac{2 - h^2}{3h^2 - 1}\right). \tag{7}$$

For $H_{CI} > 0$ and $|H| \geq H_d$, the equilibrium solutions are $m_z = \pm 1$. In this case the solution and stability condition for steady state with magnetization antialigned with the field are

$$m_z = \frac{-H}{|H|}, \qquad h_{CI} \geq \frac{\alpha}{2}\left(|h| - \frac{1}{2}\right). \tag{8}$$

This state only occurs if the magnetization is initially nearly antialigned with the applied field. The reason for its stability is that this form of the current-induced torque does not distinguish between $+\hat{z}$ and $-\hat{z}$—it merely tends to make to direct the F to the nearest available $\hat{z}$ axis, even if it is opposite to the applied field. The region for such a solution is shown in Fig. 3, labeled $\pm z$. It is seen that the applied field must be sufficiently large for this solution to be stabilized. This misaligned steady state may not be experimentally relevant, however, because it occurs only when the magnetization is initially nearly antialigned to an applied field of finite magnitude $|H| > H_d\sqrt{1/3}$.

Figure 3 shows the x and z components of the magnetization as a function of applied field and current, determined numerically. We have taken the damping $\alpha = 0.01$, and the applied field and spin transfer torque are scaled by the demagnetization field H_d. Also shown is the magnitude of the power spectrum peak of $z(t)$ (labeled "P_Z")—a nonzero value indicates a precessing solution. Also shown are the stability boundaries defined by Eqs. (3), (5), (7), and (8). The numerics verify the stability of the unusual out-of-plane and field-antialigned solutions. The conversion of the dimensionless h_{CI} into a real current density for a material with demagnetization field of 1 T is $J = (h_{CI}t) \times 3.8 \times 10^9\ \mathrm{A/cm^2}$, where t is the thickness of the F layer in nm.

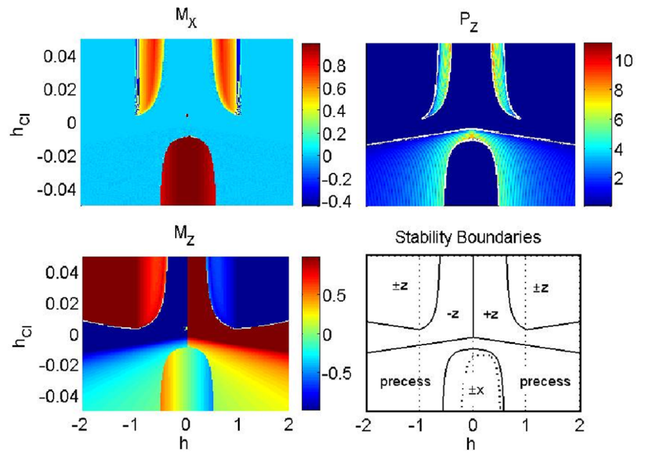

FIG. 3 (color online). Magnetic configuration (M_x, M_z) and peak of power spectrum P_z (arbitrary units) versus applied field and current. Also shown are stability boundaries found analytically (the labels $\pm x$, $\pm z$ refer also to solutions that point approximately in these directions). The stability boundary plot also shows the reduced out-of-plane solution space for negative to positive field sweep with dotted lines.

The data for each (h, h_{CI}) point in Fig. 3 are obtained beginning from an initial condition close to the solution given by Eq. (4). These equilibrium solutions are not universal attractors, and are attained for a subset of initial conditions. To see the effect of initial conditions, we have also swept the applied field from negative to positive for each applied current, using the slightly perturbed final coordinates of a trajectory as the initial condition for the next value of applied field. The out-of-plane solution space is reduced, shown by the dotted lines in Fig. 3 in the stability boundaries plot.

We now comment on the experimental possibilities of seeing these effects. In the preceding analysis, we assume that the AF is fixed. This can be accomplished by placing a large F adjacent to the AF, so that the AF is pinned via the exchange bias effect (the overall stack structure would be pinning F–AF–spacer–free F). The presence of this pinning F may influence the dynamics of the free F, but its signature should be very distinct from the influence of the AF layer on the free F. The orientation of the free F should be observable from magnetoresistance effects with the pinning ferromagnet.

A virtue of the out-of-plane F configuration is that the surface of the AF need not be single domain for its observation. As long as the magnetization of the AF is compensated and points in the plane (which is the preferred direction for NiMn [25,26]), different orientations of domains at the AF surface should cooperatively push the F out of the plane. The encouraging aspect of this proposal is that the signature of the AF current-induced torque is so unique, helping to provide a distinguished characteristic for its observation.

In summary, we show that current-induced torques are present on a F layer due to the presence of a compensated AF. The signature of these torques is an out-of-plane configuration of the F layer. We believe that observation of such a F configuration would provide unambiguous evidence of AF current-induced torques, demonstrating that these torques are a more general phenomenon than previously considered.

We would like to acknowledge very helpful conversations with Maxim Tsoi, Olle Heinonen, and Mark Stiles. This work was supported in part by Seagate Corporation and by the National Science Foundation under Grant No. DMR-0606489, and the computational work was supported by Texas Advanced Computational Center (TACC).

[1] J. C. Slonczewski, J. Magn. Magn. Mater. **159**, L1 (1996).
[2] L. Berger, Phys. Rev. B **54**, 9353 (1996).
[3] D. C. Ralph and M. D. Stiles, J. Magn. Magn. Mater. **320**, 1190 (2008).
[4] M. Tsoi *et al.*, Phys. Rev. Lett. **80**, 4281 (1998).
[5] M. Tsoi *et al.*, Nature (London) **406**, 46 (2000).
[6] J. A. Katine *et al.*, Phys. Rev. Lett. **84**, 3149 (2000).
[7] F. J. Albert *et al.*, Phys. Rev. Lett. **89**, 226802 (2002).
[8] M. R. Pufall *et al.*, Appl. Phys. Lett. **83**, 323 (2003).
[9] G. S. Beach *et al.*, Phys. Rev. Lett. **97**, 057203 (2006).
[10] J. Grollier *et al.*, Appl. Phys. Lett. **83**, 509 (2003).
[11] A. Yamaguchi *et al.*, Phys. Rev. Lett. **92**, 077205 (2004).
[12] M. Yamanouchi *et al.*, Nature (London) **428**, 539 (2004).
[13] M. Hayashi *et al.*, Phys. Rev. Lett. **96**, 197207 (2006).
[14] M. D. Stiles and A. Zangwill, Phys. Rev. B **66**, 014407 (2002).
[15] A. S. Núñez *et al.*, Phys. Rev. B **73**, 214426 (2006).
[16] P. M. Haney *et al.*, Phys. Rev. B **75**, 174428 (2007).
[17] Z. Wei *et al.*, Phys. Rev. Lett. **98**, 116603 (2007).
[18] P. M. Haney *et al.*, J. Magn. Magn. Mater. **320**, 1300 (2008).
[19] S. I. Kiselev *et al.*, Nature (London) **425**, 380 (2003).
[20] With a basis $\{|+,\uparrow\rangle, |+,\downarrow\rangle, |-,\uparrow\rangle, |-,\downarrow\rangle,\}$, the operation of sublattice interchange + time reversal has a representation

$$U = \begin{pmatrix} 0 & 1 & 0 & 0 \\ -1 & 0 & 0 & 0 \\ 0 & 0 & 0 & -1 \\ 0 & 0 & 1 & 0 \end{pmatrix}.$$

Invariance of the Hamiltonian under U implies that scattering coefficients r, t are also invariant under U, or $r = U^{-1} r U$, which implies the spin dependence is of the form described in the text.
[21] If $k_{\parallel}$ is the Bloch wave vector for a single-site unit cell of the normal metal, then the Bloch function for a 2-site unit cell is $\cos(k_{\parallel}a/2)|+\rangle - \sin(k_{\parallel}a/2)|-\rangle$. The ensuing reflected spin current has terms proportional to $\sin(2\theta)\cos^2(k_{\parallel}a/2)$, $\sin(2\theta)\sin^2(k_{\parallel}a/2)$, and $\sin(\theta) \times \sin(k_{\parallel}a)$. The $\sin(\theta)$ term vanishes after integrating over the Brouilloun zone.
[22] T. C. Schulthess *et al.*, J. Appl. Phys. **83**, 7225 (1998).
[23] P. M. Haney *et al.*, Phys. Rev. B **76**, 024404 (2007).
[24] Ya. B. Bazaliy *et al.*, Phys. Rev. B **69**, 094421 (2004).
[25] A. Sakuma, J. Magn. Magn. Mater. **187**, 105 (1998).
[26] J. S. Kasper *et al.*, J. Phys. Chem. Solids **11**, 231 (1959).